State-to-state $N_2(A\,^3\Sigma_u^+)$ energy pooling reactions. II. The formation and quenching of $N_2(B\,^3\Pi_g, v'=1\text{–}12)$

Lawrence G. Piper
Physical Sciences Inc., Research Park, P.O. Box 3100, Andover, Massachusetts 01810

(Received 14 December 1987; accepted 15 February 1988)

We have studied the state-to-state excitation of $N_2(B\,^3\Pi_g, v'=1\text{–}11)$ in energy pooling reactions between $N_2(A\,^3\Sigma_u^+, v'=0,1)$ molecules and subsequent quenching in collisions with molecular nitrogen. Excitation of vibrational levels 10, 2, and 3 appears to be much stronger than excitation of the other vibrational levels. In addition, we failed to observe any emission from $v'=12$ even though it is energetically accessible. The excitation rate coefficients are quite large, 7.7×10^{-11} cm^3 molecule^{-1} s^{-1} for the pooling of two $N_2(A, v'=0)$ molecules, and roughly a factor of three larger for energy pooling events involving $N_2(A, v'=1)$. The effective rate coefficients for electronic quenching of $N_2(B)$ by N_2 are also quite large, $\approx3\times10^{-11}$ cm^3 molecule^{-1} s^{-1}. Comparison of our quenching results with the laser-excited, real-time quenching studies of Rotem and Rosenwaks indicates agreement only within factors of 2–3.

I. INTRODUCTION

Hays and Oskam[1] investigated the temporal decay of emissions from $N_2(A\,^3\Sigma_u^+)$ and $N_2(B\,^3\Pi_g)$ in the afterglow of a pulsed discharge. They noted that the intensity of the first-positive system, $N_2(B\,^3\Pi_g$–$A\,^3\Sigma_u^+)$, varied quadratically with the intensity of the Vegard–Kaplan bands, $N_2(A\,^3\Sigma_u^+$–$X\,^1\Sigma_g^+)$, and interpreted this behavior as a sign that $N_2(B)$ was excited in the afterglow by energy pooling reactions involving $N_2(A)$. Their observations led them to assign a rate coefficient for the energy pooling process resulting in $N_2(B)$ formation of 1.1×10^{-9} cm^3 molecule^{-1} s^{-1}. One would have to assume that this number is a lower bound because their detection system could not observe $N_2(B, v'=0\text{–}2)$. Nadler *et al.*[2] discovered in 1980 that the Herman Infrared (HIR) system, which emits over the same wavelength region as $N_2(B)$, was also populated efficiently by $N_2(A)$ energy pooling. They estimated a lower limit for HIR formation of 2.5×10^{-11} cm^3 molecule^{-1} s^{-1} which they subsequently revised upward to 7×10^{-11} cm^3 molecule^{-1} s^{-1}.[3,4] They also showed that some production of the B state did indeed occur, but they were unable to estimate the rate coefficient for B-state formation because of that state's rapid quenching by nitrogen and argon.

Unpublished observations at PSI[5] in the near infrared recorded the HIR system in $N_2(A)$ energy pooling, but failed to detect significant populations of $N_2(B)$. We were thus skeptical of the magnitude of the pooling rate coefficient which Hays and Oskam had reported. The work of Nadler *et al.*[2–4] also showed convincingly that HIR production had to be similar in magnitude to the production of $N_2(B)$. Thus the present investigation was motivated in part by our desire to reconcile the conflict between Hays and Oskam's report and the observations of Nadler *et al.* as well as our own.

In part I of this investigation,[6] we studied the state-to-state excitation of $N_2(C\,^3\Pi_u, v=0\text{–}4)$ and the Herman Infrared (HIR) system, $v=2,3$, in energy pooling reactions of $N_2(A\,^3\Sigma_u^+, v'=0,1)$. We showed the excitation of $N_2(C)$ to be quite efficient for energy pooling of two $N_2(A, v'=0)$ molecules or one $v'=0$ interacting with a $v'=1$ molecule, $k=1.5\times10^{-10}$ cm^3 molecule^{-1} s^{-1}, but saw no evidence of significant formation of $N_2(C)$ when two $N_2(A, v'=1)$ molecules interacted, $k<0.5\times10^{-10}$ cm^3 molecule^{-1} s^{-1}. The Herman infrared system showed striking state specificity. Only HIR $v=3$ was excited by two $N_2(A, v'=0)$ molecules, $k=8\times10^{-11}$ cm^3 molecule^{-1} s^{-1}; a $v'=0$ and a $v'=1$ molecule combined to produce only HIR $v=2$, $k=10\times10^{-11}$ cm^3 molecule^{-1} s^{-1}; and two $N_2(A, v'=1)$ molecules appeared not to excite the Herman infrared system at all. This paper reports the extension of these investigations to $N_2(B\,^3\Pi_g)$.

II. EXPERIMENTAL

The apparatus used for these studies has been described in detail in a number of recent publications.[6–13] Basically the experiment involves generating $N_2(A)$ metastables cleanly in a discharge-flow apparatus and then monitoring spectroscopically the Vegard–Kaplan, Herman infrared and first-positive systems under constant conditions. The energy transfer reaction between metastable $Xe(^3P_{0,2})$ and N_2 produced the $N_2(A)$ metastables.[14–16] Introducing CH_4 downstream from the discharge allowed the vibrational distribution of the $N_2(A)$ to be varied so that state-specific measurements could be made.[8,17] The xenon metastables were produced in a hollow cathode discharge through a mixture of xenon and argon in a neon carrier gas. Typical flow rates through the discharge were 8, 150, and 3500 μmol s^{-1} for xenon, argon, and neon, respectively. The small argon flow was crucial to produce adequate number densities of the metastable xenon atoms. The nitrogen was then added downstream from the discharge so that we could be certain that nitrogen excitation was effected only by the energy-transfer reaction. As we show later, discharging the nitrogen along with the rare gases causes direct excitation of nitrogen in the discharge which drastically alters the $N_2(B)$ excitation magnitude and distribution in the afterglow. The reason

 0021-9606/88/116911-11$02.10

for doing the experiments in neon is that, unlike argon, neon is a relatively weak quencher of $N_2(B)$.[18,19] The distributions observed in a neon buffer when the number densities of the other gases (especially nitrogen) have been reduced to a minimum, will be relatively close to nascent. This would not be the case in an argon buffer. Not only does argon quench the $N_2(B)$ electronically, but it alters the $N_2(B)$ vibrational distribution drastically (see below). The procedure then was to repeat spectral scans of the various band systems as a function of nitrogen partial pressure. Analysis of the spectra gave populations of each vibrational level as a function of nitrogen partial pressure. Extrapolating the results to zero nitrogen partial pressure gave the nascent populations. Scans at several different neon partial pressures showed only small changes in total $N_2(B)$ excitation rate and in its vibrational distribution.

The spectra were analyzed by least-squares computer fitting as discussed previously.[8,10] We used the appropriate potential constants in Lofthus and Krupenie[20] for the Vegard–Kaplan and first-positive systems, and used the Einstein coefficients of Shemansky[21] and Shemansky and Broadfoot[22] to extract the $N_2(A)$ and $N_2(B)$ number densities. We treated the Herman infrared system empirically as described previously.[6] We also described previously our procedures for turning observed intensities into absolute photon emission rates and for correcting for the different radial density gradients of the $N_2(A)$ and the $N_2(B)$.[6]

We have expressed some concern previously that Shemansky's Einstein coefficients for $N_2(A–X)$ might be 20%–40% too large.[10,23] Furthermore, Shemansky and Broadfoot's Einstein coefficients for $N_2(B–A)$ transitions (which are the ones tabulated in Lofthus and Krupenie[20]) are somewhat questionable.[23–25] Pending resolution of these issues, however, we choose to use the commonly accepted values. We currently are investigating the $N_2(B–A)$ transition probabilities.[26] We have also found recently[26] that the potential constants of Roux *et al.*[27] fit the first-positive bands more accurately than those given in Lofthus and Krupenie.[20] The small differences do not affect the populations extracted from the spectral fitting, however.

III. RESULTS

The processes controlling the formation and destruction of $N_2(B)$ in the energy pooling of $N_2(A)$ are

$$N_2(A,v') + N_2(A,v'') \xrightarrow{k^{B,v}_{v'v''}} N_2(B,v) + N_2(X,v'''), \quad (1)$$

$$N_2(B,v) + N_2 \xrightarrow{k^{B,v}_{Q}} \text{products}, \quad (2)$$

$$N_2(B,v) \xrightarrow{k^{B,v}_{\text{rad}}} N_2(A) + h\nu, \quad (3)$$

where in the rate coefficients k, the superscript v denotes the vibrational level of the $N_2(B)$ product, the subscript v denotes the vibrational level of the $N_2(A)$ molecules, and $k^{B,v}_{\text{rad}}$ is the radiative decay rate of $N_2(B,v)$. Because the $N_2(B)$ has a lifetime on the order of microseconds,[22,25,28–30] it is in steady state within the field of view of our detector, so that we can equate its formation and destruction rates:

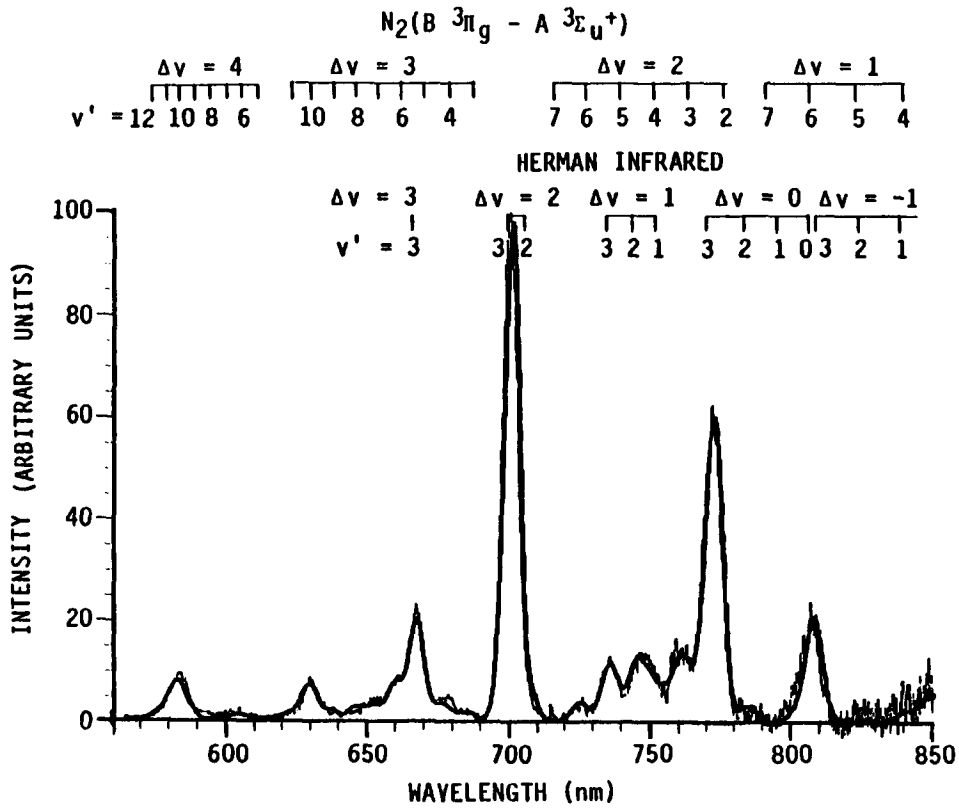

FIG. 1. Spectrum of the nitrogen Herman infrared $v' = 3$ and first-positive systems excited in the energy pooling of $N_2(A,v' = 0)$ for a nitrogen partial pressure of 0.46 Torr and a Ne pressure of 3 Torr. The experimental spectrum is the light line while the heavy line shows the synthetic best fit to the spectrum.

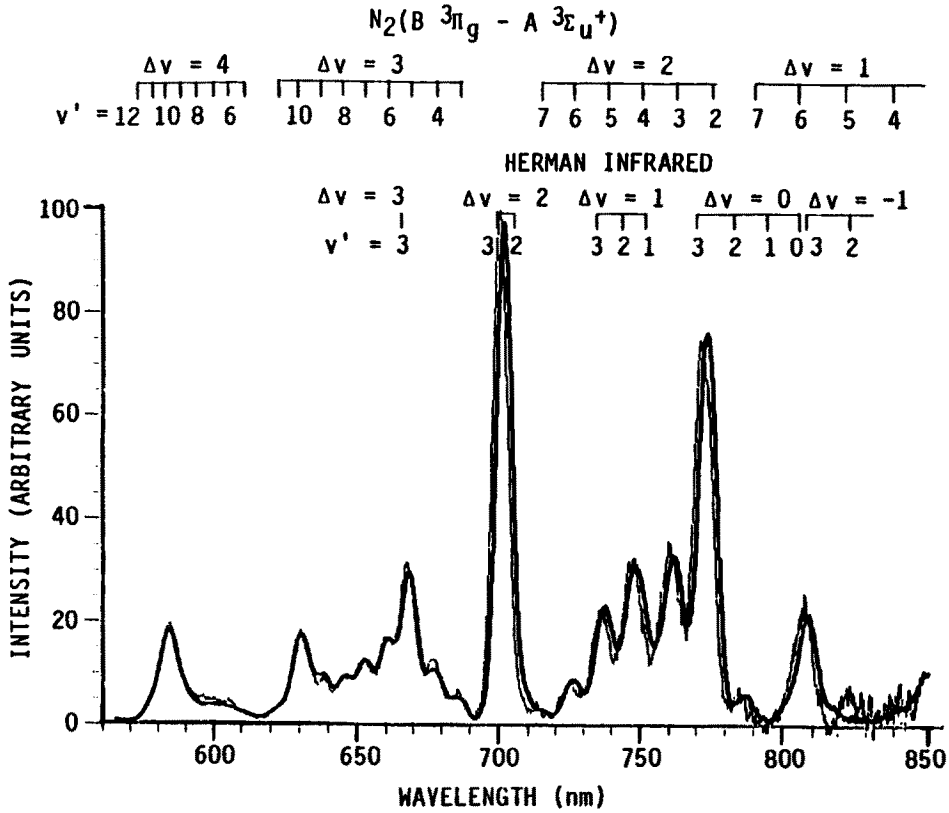

FIG. 2. Spectrum of the nitrogen Herman infrared $v' = 3$ and first-positive systems excited in the energy pooling of $N_2(A,v' = 0)$ for a nitrogen partial pressure of 0.027 Torr.

$$\frac{d[N_2(B,v)]}{dt} = 1.267 \sum_{v'} \sum_{v''} k^{B,v}_{v'v''} [N_2(A,v')][N_2(A,v'')] - \{k^{B,v}_{\text{rad}} + k^{B,v}_{Q}[N_2]\}\ [N_2(B,v)] = 0. \tag{4}$$

Thus, we have

$$[N_2(B,v)] = \frac{1.267}{k^{B,v}_{\text{rad}} + k^{B,v}_{Q}[N_2]} \sum_{v'} \sum_{v''} k^{B,v}_{v'v''} \times [N_2(A,v')]\ [N_2(A,v'')]\,. \tag{5}$$

The factor of 1.267 corrects for the differing radial density gradients of the $N_2(A)$ and $N_2(B)$.[6] For the case of energy pooling of two $N_2(A,v' = 0)$ molecules only, we have

$$[N_2(B,v)] = 1.267 \frac{k^{B,v}_{00}}{k^{B,v}_{\text{rad}}} [N_2(A,v' = 0)]^2 \times \left\{1 + \frac{k^{B,v}_{Q}}{k^{B,v}_{\text{rad}}} [N_2]\right\}^{-1}. \tag{6}$$

Rearranging this equation shows that the ratio of the square of the A state number density to the B state number density will vary linearly with the number density of the added nitrogen:

$$\frac{[N_2(A,v' = 0)]^2}{[N_2(B,v)]} = 0.789 \frac{k^{B,v}_{\text{rad}}}{k^{B,v}_{00}} + 0.789 \frac{k^{B,v}_{Q}}{k^{B,v}_{00}} [N_2]\,. \tag{7}$$

Figures 1 and 2 show spectra of the region between 500 and

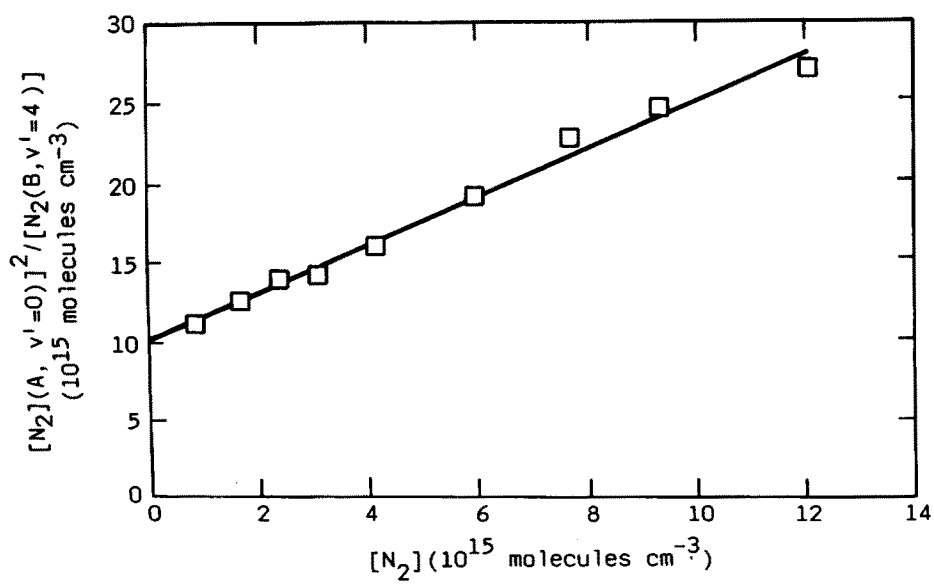

FIG. 3. Variation in the ratio of the square of the number density of $N_2(A,v' = 0)$ to that for $N_2(B,v' = 4)$ as a function of the molecular nitrogen number density.

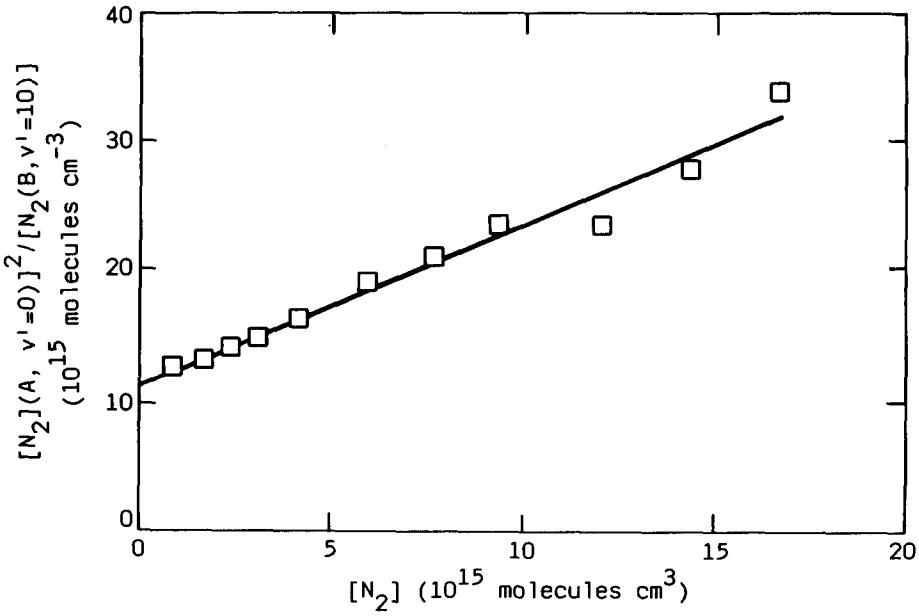

FIG. 4. Variation in the ratio of the square of the number density of $N_2(A,v'=0)$ to that for $N_2(B,v'=10)$ as a function of the molecular nitrogen number density.

850 nm with nitrogen partial pressures of 0.46 and 0.027 Torr, respectively at a constant neon pressure of 3 Torr. Clearly, the first-positive bands increase strongly with reduced nitrogen partial pressure. Figures 3 and 4 show representative data on the formation of the B state from the pooling of $N_2(A,v'=0)$ plotted according to Eq. (7). From these plots and similar ones for the other vibrational levels studied, we obtained both rate coefficients for B state formation from energy pooling (from the intercepts) and rate coefficients for quenching $N_2(B)$ by molecular nitrogen (from the slopes). The bulk of the experiments were at 3.0 Torr total pressure, but scans at 1.5 and 6 Torr gave similar vibrational distributions, and similar ratios of B-state number density to the square of the A-state number density as the data just discussed (see Fig. 5). Thus at the lowest nitrogen partial pressures studied, $N_2(B)$ quenching by the neon, argon, xenon, and CH_4 in the reactor did not appear to be large. We therefore studied the variations in B state formation from the energy pooling of vibrationally excited $N_2(A)$ under conditions comparable to those producing the minimum B-state quenching observed in the $N_2(A,v'=0)$ studies.

For these studies, we consider the system to be essentially two vibrational levels of $N_2(A)$, i.e., $v'=0$ and $v'>0$. From Eq. (5) we derive

$$\frac{[N_2(B,v)]\{1+(k_Q^{B,v}/k_{\text{rad}}^{B,v})\,[N_2]\}}{[N_2(A,v'=0)]^2} = 1.267\frac{k_{00}^{B,v}}{k_{\text{rad}}^{B,v}} + 2.534\frac{k_{0v}^{B,v}}{k_{\text{rad}}^{B,v}}\frac{[N_2(A,v'>0)]}{[N_2(A,v'=0)]} + 1.267\frac{k_{vv}^{B,v}}{k_{\text{rad}}^{B,v}}\left\{\frac{[N_2(A,v'>0)]}{[N_2(A,v'=0)]}\right\}^2, \quad (8)$$

where we have corrected only for molecular-nitrogen quenching ($\sim 10\%$ effect). Thus we can extract rates for pooling from collisions of one or both vibrationally excited $N_2(A)$ molecules from quadratic least-squares fits of the left-hand side of Eq. (8) vs the ratio $[N_2(A,v'>0)]/[N_2(A,v'=0)]$. We used the quenching-rate coefficients determined in the $N_2(A,v'=0)$ studies to correct the $N_2(B)$ number densities. Figures 2, 6, and 7 show how the spectrum between 550 and 720 nm changes as the degree of vibrational excitation in the $N_2(A)$ changes. Figures 8 and 9 show representative B-state vibrational levels plotted according to Eq. (8). The solid lines are calculated from the least-squares fit. The intercepts of these plots gave results within 10% of the $v'=0$ results determined above. These results also show that the pooling between a $v'=0$ and a $v'>0$ is somewhat faster than the pooling between two $v'=0$ molecules or between

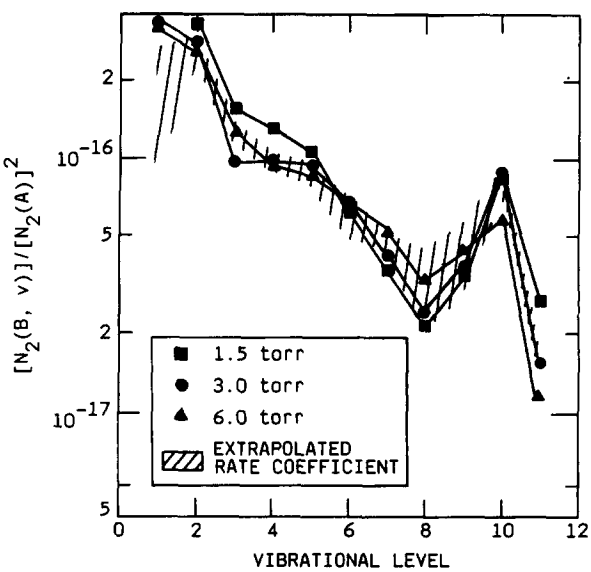

FIG. 5. Variation in $N_2(B,v)$ excited from energy pooling of $N_2(A,v'=0)$ with neon pressure.

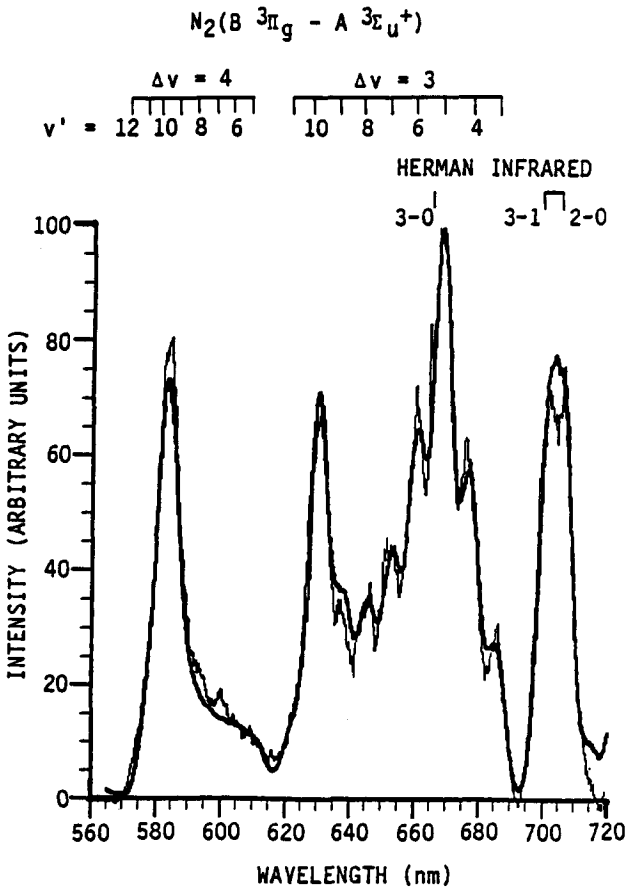

FIG. 6. Spectrum of the nitrogen Herman infrared $v' = 2,3$ and first-positive systems excited in the energy pooling of $N_2(A,v' = 0,1)$ for a nitrogen partial pressure of 38 mTorr and no added methane.

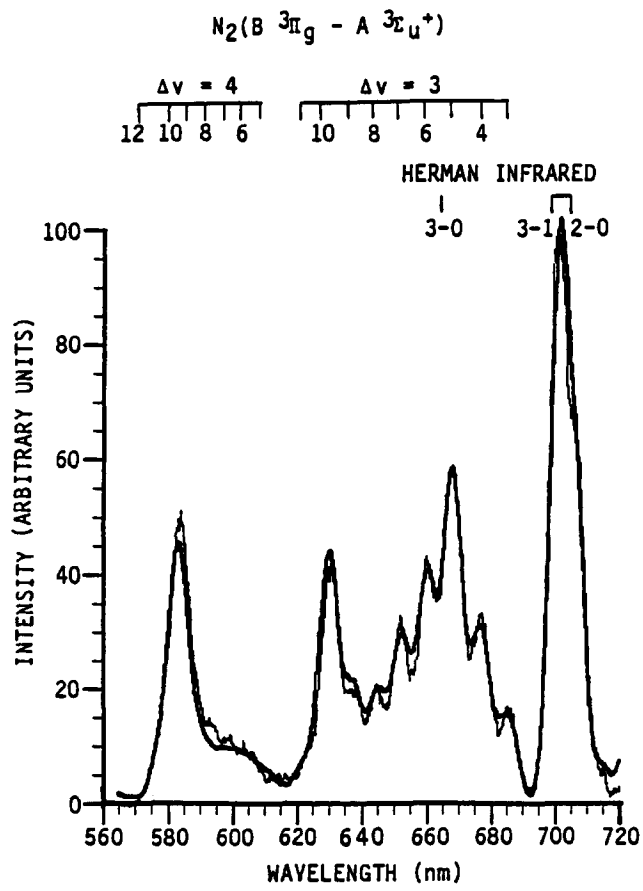

FIG. 7. Spectrum of the nitrogen Herman infrared $v' = 2,3$ and first-positive systems excited in the energy pooling of $N_2(A,v' = 0,1)$ for a nitrogen partial pressure of 38 mTorr and a methane partial pressure of 1.4 mTorr.

two $v' > 0$ molecules. Table I summarizes the rate coefficients measured, Table II the effective N_2 quenching rate coefficients.

In Table I, the rate coefficients for B-state formation are corrected for formation resulting from radiative cascade from the C-state which also is formed in $N_2(A)$ energy pooling. We multiplied the rate coefficients previously determined for C-state formation[6] by the appropriate branching ratio for radiation to the different B-state levels.[20] The terms with a common B-state level were then summed to derive the correction factors.

The error bars listed in Table I are 1σ standard deviations derived from the least-squares fits. These error bars provide, in most instances, a reasonable picture of the relative uncertainties between the measurements for the various states and also the relative uncertainty between measurements made by most other groups who will have used the same lifetimes for the A and B states. One exception will be the rate coefficient for formation of $N_2(B,v' = 1)$ for which the relative uncertainty could be as much as a factor of two or three. The only emission from this level lies at the extreme edge of the monochromator's response. The response function is rather uncertain, therefore. All other observations result from a simultaneous fit of several bands with common upper states. This fitting procedure eliminates errors due to uncertainties in the response function. In absolute terms, a roughly 40%–50% systematic uncertainty must be added to the statistical uncertainties to account for errors in the $N_2(A)$ and $N_2(B)$ lifetimes and in the air afterglow rate coefficient which was used to calibrate the optical system absolutely.

IV. DISCUSSION

Examination of the data shows several interesting results. Close to half of the B-state formation arises as a result of radiative cascade out of $N_2(C)$. The distribution of $N_2(B)$ vibrational levels excited by two $N_2(A,v' = 0)$ is independent of vibrational level except for vibrational levels two and ten, which are excited two to three times more efficiently than the other levels. As the $N_2(A)$ becomes more vibrationally excited, the $N_2(B)$ vibrational distribution begins to favor the lower vibrational levels. Under no conditions did we observe any excitation of $N_2(B,v = 12)$.

Clearly the Hays and Oskam result for the formation of $N_2(B)$ is incorrect. Their studies were performed in the afterglow of a pulsed discharge of nitrogen. A number of metastable species in addition to $N_2(A)$ will persist in the afterglow of a nitrogen discharge, and we expect that one of these other metastables is responsible for Hays and Oskam's observations. We tested this hypothesis briefly with experi-

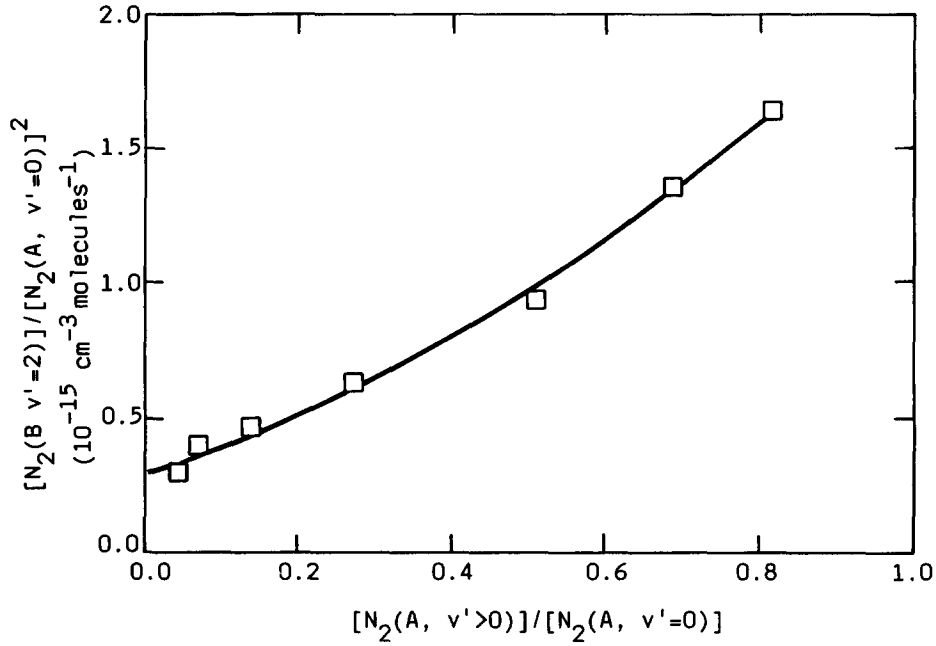

FIG. 8. Variation in the ratio of the number density of $N_2(B,v'=2)$ to the square of the number density of $N_2(A,v'=0)$ as a function of the ratio of $N_2(A)$ $v'>0$ to $v'=0$. The solid line shows the results of a quadratic least-square fit to Eq. (8).

ments in an argon buffer. We compared results when the N_2 was added in the normal fashion and when it was diverted to mix with the main argon flow upstream from the discharge. Figure 10 shows our result graphically. While discharging the nitrogen with the argon increased the $N_2(A)$ number density in the observation region by about a factor of 3, the populations of the $N_2(B)$ vibrational levels grew by a factor of 70. The HIR 3,1 band, which is relatively free from first-positive overlap, and which is therefore a good monitor of the increase in A-state pooling, grew by only a factor of 9 as would be expected. The eightfold greater increase in the B-state population than can be explained on the basis of increased A-state number densities shows clearly that discharging nitrogen directly produces metastables in addition to $N_2(A)$ which are long lived and which couple collisionally into the B state. This other state was probably responsible for Hays and Oskam's observations. Metastable $N_2(a'\ ^1\Sigma_u^-)$ molecules are formed in the discharge,[12,31] and do have enough energy to excite $N_2(B)$, but we showed them not to be responsible for $N_2(B)$ formation. Adding H_2 downstream from the discharge, but upstream from the observation region, completely eliminated $N_2(a')$ emission at 171 nm but reduced the B-state emission by less than 15%. We are currently considering other alternatives to the precursor of the enhanced B-state emission.

Adding the rate coefficients for energy pooling into $N_2(C\ ^3\Pi_u)$ and the Herman infrared system reported previously[6] to those determined here for $N_2(B\ ^3\Pi_g)$ gives a val-

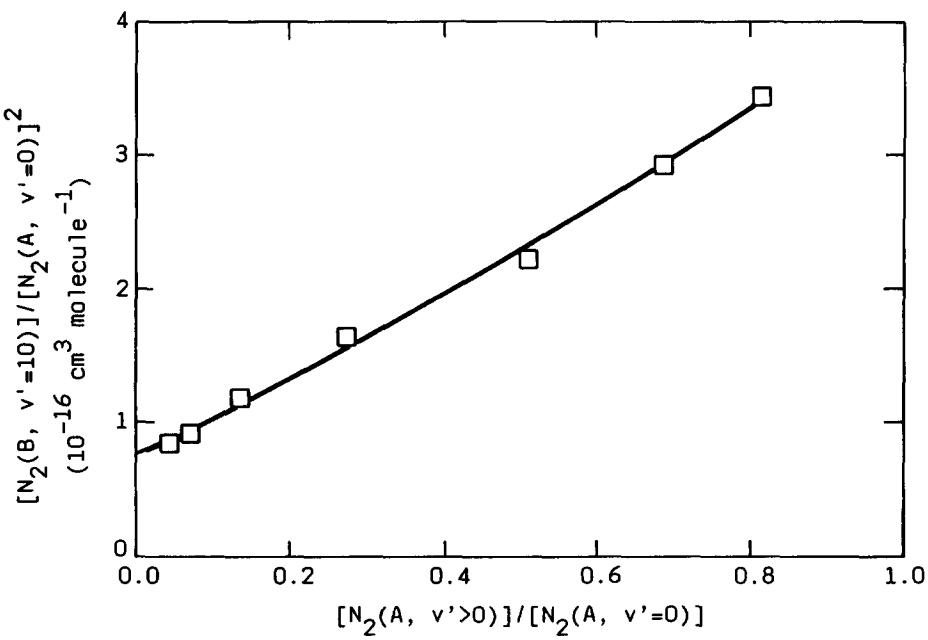

FIG. 9. Variation in the ratio of the number density of $N_2(B,v'=10)$ to the square of the number density of $N_2(A,v'=0)$ as a function of the ratio of $N_2(A)$ $v'>0$ to $v'=0$.

TABLE I. Rate coefficients for $N_2(B\,^3\Pi_g)$ formation from $N_2(A\,^3\Sigma_u^+)$ energy pooling.

	$k_{00}^{B,v}$ [a]			$k_{01}^{B,v}$			$k_{11}^{B,v}$		
$N_2(B,v')$	Observed	Cascade[b,c]	Direct	Observed	Cascade	Direct	Observed	Cascade	Direct
1	2.4 ± 0.6	3.6 ± 0.1	···	6.6 ± 1.0	3.3 ± 0.4	3.3 ± 1.4	···		
2	3.9 ± 0.2	2.3 ± 0.1	1.6 ± 0.3	5.6 ± 1.8	2.6 ± 0.4	3.0 ± 2.2	14.7 ± 4.3		
3	1.9 ± 0.1	1.5	0.4 ± 0.1	5.8 ± 0.3	1.6 ± 0.2	4.2 ± 0.5	···		
4	1.6 ± 0.1	1.1	0.5 ± 0.1	2.7 ± 1.0	1.1 ± 0.2	1.6 ± 1.2	3.8 ± 2.5		
5	1.5 ± 0.1	0.8	0.7 ± 0.1	2.2 ± 0.6	0.6 ± 0.1	1.6 ± 0.7	4.5 ± 1.3		
6	1.1 ± 0.1	0.5	0.6 ± 0.1	1.7 ± 0.2	0.4 ± 0.1	1.3 ± 0.3	1.5 ± 0.5		
7	0.9 ± 0.1	0.3	0.6 ± 0.1	1.6 ± 0.1	0.3	1.3 ± 0.1	···		
8	0.6 ± 0.1	0.2	0.4 ± 0.1	1.3 ± 0.1	0.2	1.1 ± 0.1	···		
9	0.9 ± 0.1	0.1	0.8 ± 0.1	1.0 ± 0.4	0.1	0.9 ± 0.4	1.6 ± 1.0		
10	1.8 ± 0.1		1.8 ± 0.1	2.8 ± 0.5		2.8 ± 0.5	1.3 ± 1.1		
11	0.32 ± 0.04		0.32 ± 0.04	0.4 ± 0.2		0.4 ± 0.2	1.0 ± 0.5		
$N_2(B)$ Total			7.7 ± 1.1			21.5 ± 7.6	28 ± 11		

[a] Rate coefficients are in units of 10^{-11} cm^3 molecules^{-1} s^{-1}.
[b] Cascade corrections are based upon the results of Ref. 6.
[c] If no cascade error bar is listed, it is less than ± 0.05.

ue of 3.0 and 4.7×10^{-10} cm^3 molecule^{-1} s^{-1} for energy pooling of two $N_2(A,v'=0)$ and of $N_2(A,v'=0)+N_2(A,v'=1)$, respectively. These numbers represent a lower limit to the total energy pooling rate coefficient, because unobserved states might be involved, and also because we have not been able to evaluate the contributions of $N_2(B,v'=0)$ formation. Since vibrational levels one through eight are all formed at least 50% by radiative cascade from the C state, we would expect $N_2(B,v'=0)$ to follow suit. This would raise the total pooling rate coefficient by less than 10%. The formation of unobserved states cannot readily be assessed. A number of states are available, most notably the $W\,^3\Delta_u$ and $B'\,^3\Sigma_u^-$ states. We do see the 5–1 band of the B'–B system at 825 nm, but cannot tell whether it is formed directly or by collisions between $N_2(B)$ and N_2. In addition, we have observed a small amount of emission in the 140 to 180 nm region which is probably from the Lyman–Birge–Hopfield system, but the intensities are much too weak to resolve for an adequate identification. We would therefore not expect the singlet states to form a significant exit channel.

Various groups have used a Franck–Condon model to try to rationalize their energy transfer results.[4,32–35] The thinking is that the energy-transfer rate coefficients should scale roughly as

$$k \sim q_1 q_2 e^{-|\Delta E|/kT}, \tag{9}$$

where q_1 and q_2 are the Franck–Condon factors coupling initial and final states in the energy-transfer process and ΔE is the energy defect for the transfer process. Our experimental results comprise an extensive set of state-to-state energy-transfer rate coefficients and therefore can provide an arduous test of this model. Table III compares experimental and model results. The model results were normalized to give the same rate coefficient as determined experimentally for the energy-pooling process involving two $N_2(A,v'=0)$

TABLE II. Rate coefficients[a] for $N_2(B)$ quenching by N_2.

N_2 B,v	This work[a]	Reference 36	Reference 37	Reference 40	Reference 19[b]	References 38 and 39	Reference 41
1	1.0 ± 0.8	0.8	~1		1.2	⩾0.77	0.22 ± 0.02
2	0.8 ± 0.1	1.2	1.9 ± 0.2		3.6	⩾0.89	0.32 ± 0.02
3	3.0 ± 0.2	2.1	1.7 ± 0.2		9.0		
4	2.4 ± 0.1	1.9	1.8 ± 0.2		4.3		
5	2.6 ± 0.1	1.8	2.3 ± 0.2		6.8		
6	2.1 ± 0.3	1.8	4.1 ± 0.4		···		
7	6.4 ± 0.3	2.4	6.6 ± 0.4		···		
8	8.0 ± 2.4		7.2 ± 0.4		7.5		
9	7.0 ± 1.2		9.8 ± 1.0	0.9	2.8		
10	2.3 ± 0.2		6.3 ± 0.8	2.8	5.3	4.4 ± 0.9	
11	2.8 ± 0.2		2.0 ± 0.3	7.2	···		

[a] Units 10^{-11} cm^3 molecule^{-1} s^{-1}.
[b] Based on two-state coupling model.

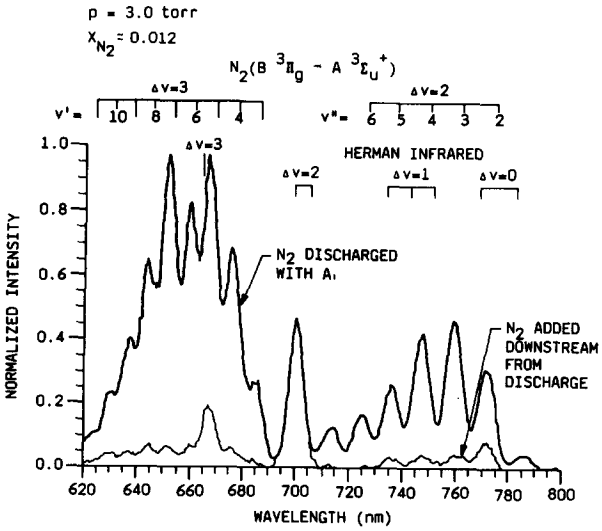

FIG. 10. Spectra of HIR $v' = 3$ and N_2 first-positive systems when the $N_2(A)$ is formed by direct discharge of the N_2 with the argon and when it is formed in the conventional manner by adding the N_2 downstream from the discharge. The two spectra were normalized so that the Herman infrared 3,1 bands at 703 nm would coincide.

molecules. Examination of the table shows that the model fails to predict the $N_2(B,v)$ distributions from the various energy-transfer processes even qualitatively. Nor does it predict how the rate coefficient for producing a given vibrational level of $N_2(B)$ will vary as the $N_2(A)$ becomes vibrationally excited. Previously we have noted this failure of the Franck–Condon model to predict $N_2(C,v)$ distributions from $N_2(A)$ energy pooling[6] and $NO(A,v)$ distributions excited in the energy transfer reaction between $N_2(A,v'')$ and NO.[10]

TABLE III. Comparison between observed energy pooling rate coefficients and those predicted by a Franck–Condon model.

	$k_{00}^{B,v}$ [a]		$k_{01}^{B,v}$ [a]		$k_{11}^{B,v}$ [a]	
$N_2(B,v')$	Model[b]	Observed	Model[b]	Observed	Model[b]	Observed
1	0.03	···	12.4	3.3	0.06	···
2	0.3	1.6	16.3	3.0	27.2	14.7
3	1.0	0.4	10.6	4.2	82.1	···
4	2.9	0.5	3.7	1.6	73.2	3.8
5	3.0	0.7	5.2	1.6	24.4	4.5
6	0.14	0.6	5.5	1.3	14.1	1.5
7	0.003	0.6	0.24	1.3	15.3	···
8	0.004	0.4	0.05	1.1	6.5	···
9	0.06	0.8	0.025	0.9	0.6	1.6
10	0.06	1.8	0.8	2.8	···	1.3
11	0.02	0.3	2.9	0.4	0.2	1.0
12	0.14	···	0.044	···	0.02	···
$N_2(B)$ Total	7.7	7.7	58.1	21.5	243.1	28.0

[a] Units are 10^{-11} cm^3 molecule^{-1} s^{-1}.

[b] The model calculations have been normalized to give the same total rate coefficient for two $N_2(A,v' = 0)$ molecules as was observed experimentally.

Table II lists the rate coefficients for electronic quenching of $N_2(B,v)$ determined in this study along with several other sets of values in the literature. Agreement with the measurements of Mitchell[36] and of Shemansky,[37] both of whom excited $N_2(B,v)$ by electron impact, is fair as is agreement with Gartner and Thrush's[38,39] measurements in a recombining N-atom afterglow. Agreement with Becker *et al.*'s[40] afterglow observations and the kinetic absorption spectroscopy determination of Dreyer and Perner[41] following excitation of nitrogen by relativistic electrons is not so good. All of these numbers are effective two-body quenching rate coefficients. The actual processes involved are much more complex. The $B\ ^3\Pi_g$ state of nitrogen is coupled collisionally into a number of other nested electronic states including the $A\ ^3\Sigma_u^+$, $B'\ ^3\Sigma_u^-$, $W^3\Delta_u$, and perhaps various states of the singlet manifold including $X\ ^1\Sigma_g^+$.[18,19,35,42–44] Thus the quenching is actually a complex process which involves shuttling energy back and forth between the various states involved. Sadeghi and Setser[18,42] and Rotem *et al.*[19,43,44] have demonstrated this coupling between the states unequivocally. These groups have excited specific vibrational levels of the $B\ ^3\Pi_g$ state by laser pumping $A\ ^3\Sigma_u^+$–state molecules. Subsequent to the laser pumping they observe emission from $B'\ ^3\Sigma_u^-$–state levels, and lower vibrational levels of the $B\ ^3\Pi_g$ state, as well as pressure-dependent, multiexponential decays of the fluorescence from the initially populated level. In most cases the fluorescence decays can be separated into two pressure dependent components, one fairly fast, and the other quite slow. The rapidly decaying component represents coupling into a reservoir state which is in equilibrium with the initially pumped level. Generally the $W^3\Delta_u$ state is identified as the primary reservoir state.

Sadeghi and Setser[18] and Rotem *et al.*[19,43,44] tried to describe their observations using the two-state coupling model given by Yardley.[45] We derived a steady-state expression consistent with this model to allow comparison of our observations with those of Rotem and Rosenwaks.[19]

The following reactions describe the model:

$$N_2(A) + N_2(A) \xrightarrow{k_{ep}} N_2(B) + N_2(X), \tag{10}$$

$$N_2(B) + N_2(X) \underset{k_{WB}}{\overset{k_{BW}}{\rightleftarrows}} N_2(W) + N_2(X), \tag{11}$$

$$N_2(B) + N_2(X) \xrightarrow{k_Q^B} 2N_2(X), \tag{12}$$

$$N_2(B) \xrightarrow{k_r^B} N_2(A) + h\nu, \tag{13}$$

$$N_2(W) + N_2(X) \xrightarrow{k_Q^W} 2N_2(X), \tag{14}$$

$$N_2(W) \xrightarrow{k_r^W} N_2(B) + h\nu, \tag{15}$$

where we have assumed W as the reservoir state. The B', A, and perhaps even the X state could also be reservoir states. For simplicity's sake, however, we designate only one reservoir state. This set of equations defines the following rates:

$$R_f = k_{ep}[N_2(A)]^2, \tag{16}$$

$$R_1 = k_r^B + k_Q^B[N_2], \tag{17}$$

$$R_2 = k_{BW}[N_2], \tag{18}$$

$$R_{-2} = k_{WB}[N_2], \tag{19}$$

$$R_3 = k_r^W + k_Q^W[N_2]. \tag{20}$$

The rate of formation of state W is

$$\frac{d[W]}{dt} = R_2[B] - (R_{-2} + R_3)[W]. \tag{21}$$

Under steady-state conditions we obtain

$$[W] = R_2[B]/(R_{-2} + R_3). \tag{22}$$

The rate of formation of state B is

$$\frac{d[B]}{dt} = R_f - (R_1 + R_2)[B] + R_{-2}[W]. \tag{23}$$

Under steady-state conditions, with the inclusion of Eq. (22) above, Eq. (23) becomes

$$R_f/[B] = [(R_1 + R_2)(R_{-2} + R_3) - R_2R_{-2}]/(R_{-2} + R_3). \tag{24}$$

The two-state coupling model of Yardley explains biexponential decays of state B as

$$\frac{[B](t)}{[B](t=0)} = A_1 e^{-\lambda_1(t)} + A_2 e^{-\lambda_2(t)}. \tag{25}$$

Under conditions such that $\lambda_1 \gg \lambda_2$ the following expressions apply:

$$\lambda_1 \approx R_2 + R_{-2} = k_{BW}P(1+\chi), \tag{26}$$

$$\lambda_2 \approx \frac{(R_1 + R_2)(R_{-2} + R_3) - R_2R_{-2}}{R_2 + R_{-2}}, \tag{27}$$

$$\approx \frac{k_r^B\chi + k_r^W}{1+\chi} + \frac{k_Q^B\chi + k_Q^W}{1+\chi}P, \tag{28}$$

$$\chi = K_{eq}^{-1} = \frac{k_{WB}}{k_{BW}} = \frac{A_2}{A_1}. \tag{29}$$

Combining Eqs. (24) and (27) gives

$$\frac{R_f}{[B]} = \lambda_2\left(\frac{R_2 + R_{-2}}{R_{-2} + R_3}\right) = \lambda_2\left[\frac{1+\chi}{\chi + (R_3/R_2)}\right]. \tag{30}$$

Applying expression (28) for λ_2 gives

$$\frac{R_f}{[B]} = \frac{k_r^B\chi + k_r^W}{\chi + (R_3/R_2)} + \frac{k_Q^B\chi + k_Q^W}{\chi + (R_3/R_2)}P. \tag{31}$$

This expression has a form similar to Eq. (7) which describes the quenching of $N_2(B)$. The product of the ratio of the factor multiplied by P to the constant term in Eq. (31) times k_r^B gives the effective rate coefficient for quenching, based upon rates determined experimentally from the laser-pumping experiments, i.e.,

$$k_Q^{\text{eff}} = \frac{k_Q^B\chi + k_Q^W}{k_r^B\chi + k^W}k_r^B. \tag{32}$$

Rotem and Rosenwaks[19] studied vibrational-level dependent decays as a function of nitrogen pressure. The effective rate coefficient of their slowly decaying component is

$$k_s = \frac{d\lambda_2}{dp} = \frac{k_Q^B\chi + k_Q^W}{1+\chi}. \tag{33}$$

This expression combines with Eq. (31) to give

$$k_Q^{\text{eff}} = \frac{k_s(1+\chi)}{k_r^B\chi + k_r^W}k_r^B. \tag{34}$$

We list values of k_Q^{eff} based upon their measurements of k_s and χ in Table II. We used the radiative lifetimes of $N_2(B)$ and $N_2(W)$ calculated by Werner *et al.*[24] to derive the k_Q^{eff} values listed. The calculation assumes that the coupling is with the vibrational level of the $W\,^3\Delta_u$ state which is closest in energy resonance to the vibrational level of $B\,^3\Pi_g$ considered. Clearly this approximation is somewhat simplistic and may account for the rather mediocre agreement between our measured, effective quenching rate coefficients, and those we calculate based upon the two-state coupling model and Rotem and Rosenwaks' experimental results. Under the circumstances, perhaps a factor of 2–3 agreement is acceptable. The coupling is probably too complex to be explained by *only* a two-state model. The ultimate test of any model used to describe phenomena on a microscopic scale is that it be able to reproduce effects observed in global experiments. The two-state model achieves this goal only in part, and appears to need further development.

The microscopic details of the quenching processes depend strongly upon the quenching partner. Nitrogen appears to quench electronic energy out of all levels at roughly comparable rates, and thereby shows little evidence of effecting vibrational relaxation within the $N_2(B)$ vibrational manifold.[46] Argon, on the other hand, is much less efficient than nitrogen at quenching $B\,^3\Pi_g$ manifold electronically, but it rather efficiently alters the vibrational distribution.[40,47] Figure 11 demonstrates this point dramatically. The spectrum in Fig. 11(a) for which the nitrogen partial pressure is 0.21 Torr, shows fairly strong first-positive band attenuation relative to the unquenched Herman infrared band at 703 nm. The vibrational distribution, however, is quite similar to that in Fig. 6 which was taken under conditions of sufficiently low nitrogen partial pressure that electronic quenching is minimal. Figure 11(b) shows that reducing the nitrogen partial pressure, so as to eliminate N_2 quenching effects, results in a much stronger first-positive system intensity. In argon, however, the vibrational-level distribution is drastically altered. Raising the argon pressure further, as shown in Figs. 11(c) and 11(d), does result in some reduction in the first-positive system intensity, but more noticeable is the continual shifting of the vibrational distribution. Especially interesting in Fig. 11(d), which is with 10 Torr of argon, is that the vibrational distribution appears to hang up in $v' = 8$. The apparent electronic quenching by argon in Figs. 11(c) and 11(d) compared to Fig. 11(b) might result only from shifting the $B\,^3\Pi_g$ population into vibrational levels $v' = 0$–2 which do not emit in the spectral region observed. The observations would have to be extended into the infrared to clarify this point. Clearly $N_2(B\,^3\Pi_g)$ quenching is an extremely complex process, and simple models such as implied by Eq. (7) or even Eq. (31) are not completely adequate.

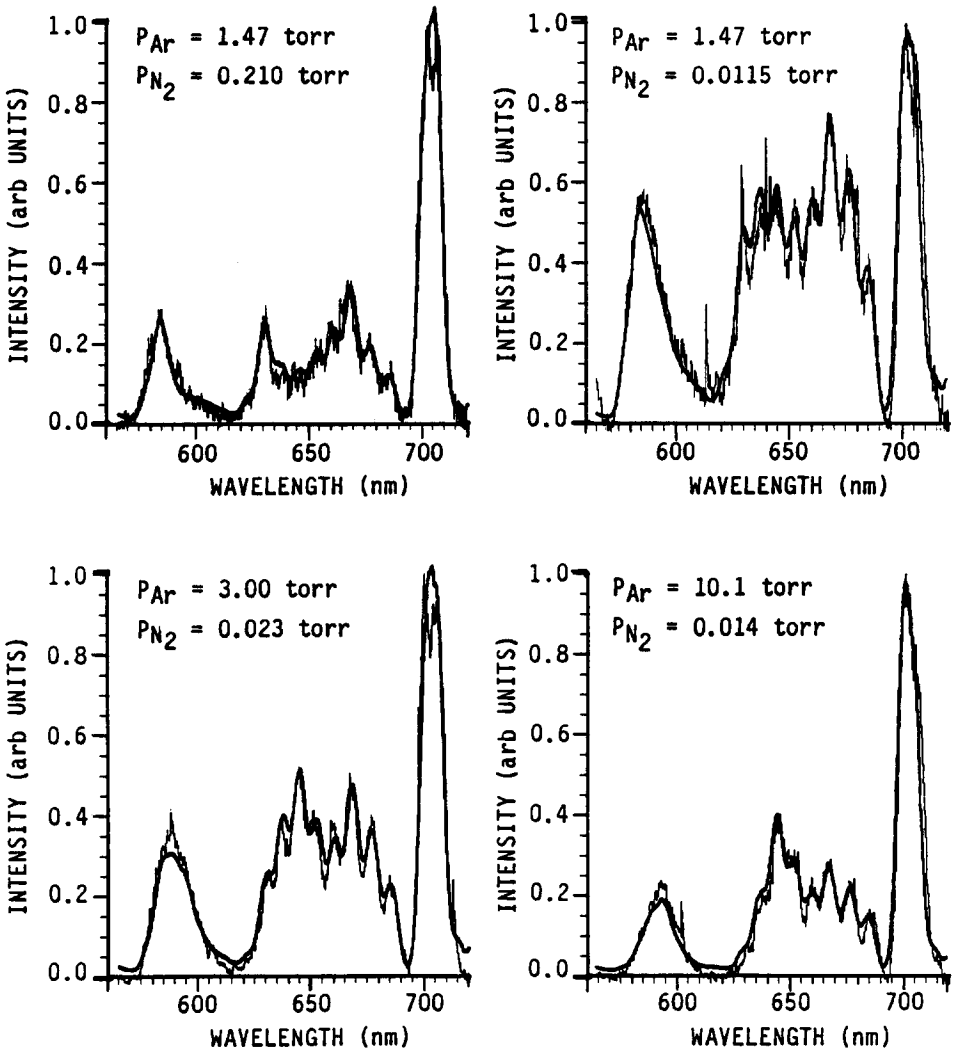

FIG. 11. Variation in the $N_2(B,A)$ spectrum produced in $N_2(A)$ energy pooling with changes in nitrogen and argon partial pressures. The solid line is the best fit synthetic spectrum.

V. SUMMARY AND CONCLUSIONS

While our results indicate clearly that the formation of $N_2(B\,^3\Pi_g)$ in $N_2(A\,^3\Sigma_u^+)$ energy-pooling reactions is efficient, $k \sim 10^{-10}$ cm^3 molecule^{-1} s^{-1}, it is an order of magnitude less efficient than previous reports.[1] Our investigations indicate that the earlier measurements were made in the presence of additional N_2 metastables which also are collisionally coupled to $N_2(B)$. The sum of the rate coefficients for $N_2(B)$ excitation reported here and those for $N_2(C)$ and N_2(HIR) reported previously[6] give a lower limit to the total $N_2(A)$ energy-pooling rate coefficient of $3\text{–}5\times10^{-10}$ cm^3 molecule^{-1} s^{-1} depending on the $N_2(A)$ vibrational level distribution. This figure is substantially below the previously reported values of $1\text{–}3\times10^{-9}$ cm^3 molecule^{-1} s^{-1}. This discrepancy could be reduced somewhat by including unobserved nitrogen states such as $B'\,^3\Sigma_u^-$ and $W\,^3\Delta_u$. Including these states will require spectral observations well out into the infrared. The 0,0 transitions of $B'\,^3\Sigma_u^- - B\,^3\Pi_g$ lies at 1528 nm while the 2,0 and 1,0 transitions of $W\,^3\Delta_u - B\,^3\Pi_g$ are at 3320 and 6430 nm, respectively. The 0,0 transition of the W–B system is too far into the infrared for conventional detectors. Nevertheless, a search in the infrared for B'–B transitions, as well as transitions from the higher vibrational levels of the W state appears to be the next important step in unraveling $N_2(A)$ energy pooling.

Our observations of state-to-state transfer rates provide an important test for the Franck–Condon model which has been invoked so enthusiastically in recent years. We have been unable to find even qualitative agreement between this model and our observations on $N_2(A)$ energy pooling, both in this work and in our experiments reported in Ref. 6. Neither did our state-to-state measurements on the excitation of $NO(A\,^2\Sigma^+)$ by $N_2(A)$[10] provide any support for this model. The failure of the Franck–Condon model to describe these systems is especially intriguing because it apparently describes reasonably well some aspects of the excitation of sulfur-containing molecules by $N_2(A)$.[48,49]

ACKNOWLEDGMENTS

This work was supported partially by Contract No. F19628-85-C-0032 with the Air Force Geophysics Laboratory, who are sponsored by the Defense Nuclear Agency under Project 5A, Task 5A, work unit 00115, and by the Air Force Office of Scientific Research under Task 2310G4, and also partially by Contract No. F19628-85-C-0076 with the Air Force Weapons Laboratory. We appreciate illuminating

discussions with Professor Donald W. Setser of Kansas State University and Dave Green and Terry Rawlins of PSI and the invaluable data analysis capabilities of Margrethe DeFaccio.

[1]G. N. Hays and H. J. Oskam, J. Chem. Phys. **59**, 1507 (1973).
[2]I. Nadler, D. W. Setser, and S. Rosenwaks, Chem. Phys. Lett. **72**, 536 (1980).
[3]I. Nadler, A. Rotem, and S. Rosenwaks, Chem. Phys. **69**, 375 (1982).
[4]I. Nadler and S. Rosenwaks, J. Chem. Phys. **83**, 3932 (1985).
[5]L. G. Piper (unpublished results).
[6]L. G. Piper, J. Chem. Phys. **88**, 321 (1988).
[7]L. G. Piper, G. E. Caledonia, and J. P. Kennealy, J. Chem. Phys. **75**, 2847 (1981).
[8]L. G. Piper, W. J. Marinelli, W. T. Rawlins, and B. D. Green, J. Chem. Phys. **83**, 5602 (1985).
[9]L. G. Piper and W. T. Rawlins, J. Phys. Chem. **90**, 320 (1986).
[10]L. G. Piper, L. M. Cowles, and W. T. Rawlins, J. Chem. Phys. **85**, 3369 (1986).
[11]L. G. Piper, M. E. Donahue, and W. T. Rawlins, J. Phys. Chem. **91**, 3883 (1987).
[12]L. G. Piper, J. Chem. Phys. **87**, 1625 (1987).
[13]L. G. Piper, G. E. Caledonia, and J. P. Kennealy, J. Chem. Phys. **74**, 2888 (1981).
[14]D. W. Setser, D. H. Stedman, and J. A. Coxon, J. Chem. Phys. **53**, 1004 (1970).
[15]D. H. Stedman and D. W. Setser, Chem. Phys. Lett. **2**, 542 (1968).
[16]N. Sadeghi and D. W. Setser, Chem. Phys. Lett. **82**, 44 (1981).
[17]J. M. Thomas, J. B. Jeffries, and F. Kaufman, Chem. Phys. Lett. **102**, 50 (1983).
[18]N. Sadeghi and D. W. Setser, J. Chem. Phys. **79**, 2710 (1983).
[19]A. Rotem and S. Rosenwaks, Opt. Engineering **22**, 564 (1983).
[20]A. Lofthus and P. H. Krupenie, J. Phys. Chem. Ref. Data **6**, 287 (1977).
[21]D. E. Shemansky, J. Chem. Phys. **51**, 689 (1969).
[22]D. E. Shemansky and A. L. Broadfoot, J. Quant. Spectrosc. Radiat. Transfer **11**, 1385 (1971).
[23]L. G. Piper, S. J. Davis, H. C. Murphy, W. P. Cummings, L. P. Walkauskas, M. A. DeFaccio, L. M. Cowles, W. T. Rawlins, W. J. Marinelli, and B. D. Green, PSI-076/TR-593 under Air Force Weapons Laboratory Contract No. F29601-84-C-0076 (1987).
[24]H. J. Werner, J. Kalcher, and E. A. Reinsch, J. Chem. Phys. **81**, 2420 (1984).
[25]E. E. Eyler and F. M. Pipkin, J. Chem. Phys. **79**, 3654 (1983).
[26]L. G. Piper, K. W. Holtzclaw, B. D. Green, and W. A. M. Blumberg, Bull. APS **33**, 155 (1988); and manuscript in preparation.
[27]F. Roux, F. Michaud, and J. Verges, J. Mol. Spectrosc. **97**, 253 (1983).
[28]M. Jeunehomme, J. Chem. Phys. **45**, 1805 (1966).
[29]T. A. Carlson, N. Duric, P. Erman, and M. Larsson, Phys. Scr. **19**, 25 (1979).
[30]R. F. Heidner III, D. G. Sutton, and S. N. Suchard, Chem. Phys. Lett. **37**, 243 (1976).
[31]M. F. Golde, Chem. Phys. Lett. **31**, 348 (1975).
[32]F. Deperesinka, J. A. Beswick, and A. Tramer, J. Chem. Phys. **71**, 2477 (1979).
[33]D. H. Katayama, T. A. Miller, and V. E. Bondybey, J. Chem. Phys. **69**, 3602 (1978).
[34]R. D. Coombe and C. H.-T. Lam, J. Chem. Phys. **80**, 3106 (1984).
[35]D. S. Richards and D. W. Setser, Chem. Phys. Lett. **136**, 215 (1987).
[36]K. B. Mitchell, J. Chem. Phys. **53**, 1957 (1970).
[37]D. E. Shemansky, J. Chem. Phys. **64**, 565 (1976).
[38]E. M. Gartner and B. A. Thrush, Proc. R. Soc. London Ser. A **346**, 103 (1975).
[39]E. M. Gartner and B. A. Thrush, Proc. R. Soc. London Ser. A **346**, 121 (1975).
[40]K. H. Becker, E. H. Fink, W. Groth, W. Jud, and D. Kley, Discuss. Faraday Soc. **53**, 35 (1972).
[41]J. W. Dreyer and D. Perner, Chem. Phys. Lett. **16**, 169 (1972).
[42]N. Sadeghi and D. W. Setser, Chem. Phys. Lett. **77**, 304 (1981).
[43]A. Rotem, I. Nadler, and S. Rosenwaks, J. Chem. Phys. **76**, 2109 (1982).
[44]A. Rotem, I. Nadler, and S. Rosenwaks, Chem. Phys. Lett. **83**, 281 (1981).
[45]J. T. Yardley, *Introduction to Molecular Energy Transfer* (Academic, New York, 1980).
[46]B. D. Green, W. J. Marinelli, L. G. Piper, and W. Blumberg (in preparation).
[47]R. L. Brown, J. Chem. Phys. **52**, 4604 (1970).
[48]D. S. Richards and D. W. Setser, Chem. Phys. Lett. **136**, 215 (1987).
[49]D. Z. Cao and D. W. Setser, J. Phys. Chem. **92**, 1169 (1988).